

International Journal of Intelligent Systems Technologies and Applications

ISSN online: 1740-8873 - ISSN print: 1740-8865
<https://www.inderscience.com/ijista>

Design and development of political rider competitive swarm optimiser enabled deep learning model for air quality detection

Deepika Dadasaheb Patil, T.C. Thanuja, Bhuvaneshwari C. Melinamath

DOI: [10.1504/IJISTA.2024.10060984](https://doi.org/10.1504/IJISTA.2024.10060984)

Article History:

Received:	07 February 2022
Last revised:	25 July 2023
Accepted:	04 September 2023
Published online:	05 February 2024

Design and development of political rider competitive swarm optimiser enabled deep learning model for air quality detection

Deepika Dadasaheb Patil*

Department of Computer Science and Engineering,
Vishveshvaraya Technological University,
Belgavi, India
and
Sanjay Ghodawat University,
Kolhapur, India
Email: deepikadadasaheb@gmail.com
*Corresponding author

T.C. Thanuja

Department of VLSI and Embedded System,
Visvesvaraya Technological University,
Belagavi, India
Email: tcthanuja@gmail.com

Bhuvaneshwari C. Melinamath

Department of Computer Science and Engineering,
BMSIT&M College,
Bangalore, India
Email: melinamathb@yahoo.com

Abstract: The air quality prediction process is a more significant one for air pollution prevention and management because air pollution becomes crueller. The precise identification of air quality has become a more significant concern for controlling air pollution. Recently, the weight of particulate matter (PM) on the human physical condition has become an important research area. In this paper, the political rider competitive swarm optimiser (PRCSO)-based deep recurrent neural network (DRNN) algorithm is devised for air quality and carbon monoxide prediction. The missing value imputation scheme is employed to perform pre-processing. Moreover, technical indicators and location information are extracted for the prediction process. The DRNN is employed for prediction, which is trained by the PRCSO and the training process is performed based on every location independently. The PRCSO-based DRNN outperforms existing techniques in terms of mean square error (MSE) of 0.0313, and mean absolute percentage error (MAPE) of 3.08%.

Keywords: air quality prediction; carbon monoxide prediction; deep recurrent neural network; DRNN; political optimiser; relative strength index; mean square error; MSE; mean absolute percentage error; MAPE.

Reference to this paper should be made as follows: Patil, D.D., Thanuja, T.C. and Melinamath, B.C. (2024) 'Design and development of political rider competitive swarm optimiser enabled deep learning model for air quality detection', *Int. J. Intelligent Systems Technologies and Applications*, Vol. 22, No. 1, pp.77–104.

Biographical notes: Deepika Dadasaheb Patil is an Assistant Professor in Department of Computer Science and Engineering at Sanjay Ghodawat University Kolhapur, Maharashtra, India. She received her Bachelor's and Master's in Computer Science and Engineering from Visvesvaraya Technological University, Belagavi Karnataka, India in 2009 and 2015. Her research interests include artificial intelligence and machine learning techniques.

T.C. Thanuja is a Professor in Department of Electronics and Communication Engineering, Visvesvaraya Technological University Belagavi, Karnataka, India. She earned her Bachelor's and Master's in Electronics and Communication Engineering from Bangalore University, Karnataka and PhD in Electronics and Communication Engineering from Avinashilingam University for Women, Coimbatore Tamilnadu in 2010. Her research area is image processing and VLSI design. She has more than 50 publications in reputed international journals and conferences. She is a life member of professional bodies like ISTE, IACSIT, IMAPS and IETE.

Bhuvaneshwari C. Melinamath is a Professor in Department of Computer Science and Engineering in BMSIT&M College of Engineering Bangalore India. She earned her Bachelor's and Master's in Computer Science and Engineering from Visvesvaraya Technological University, Belagavi Karnataka, India and PhD in Computer Science and Engineering from Central University Hyderabad. Her research area is natural language processing. She has more than 30 publications in reputed international journals and conferences. She is a life member of professional bodies like ISTE and IETE.

1 Introduction

The air quality forecast is one of the major significant processes for managing air pollution in metropolitan areas. However, the air quality prediction model has various challenges, including instability of data source, variation of pollutant concentration and high improbability. Thus, the above limitations and challenges faced by existing air quality prediction techniques are considered major stimulation to develop a novel model, termed the political rider competitive swarm optimiser (PRCSO)-based deep recurrent neural network (DRNN) approach. In previous days, the fast growth of urbanisation as well as industrialisation increases air pollutant concentrations around the world (Ma et al., 2019). In urban regions, air contamination is a familiar concern for humans. The rapid increment of the population in cities, as well as the developing level of motorisation, directs to rising traffic volume. Meanwhile, the thickening of urban constructions decreases freshening and also enlarges the surface porosity, which effectively reduces the wind effect in contamination evacuation. The Poland city is established in the 10th century and has 641,000 residents at present. Moreover, about 15,000 vehicles are calculated to move on city roads daily (Chalfen and Kamińska, 2018;

Espinosa et al., 2021). Air pollution becomes a significant health issue, which affects millions of humans globally. Additionally, several reports state that 4.2 million deaths were recognised for controlling outdoor air pollution in the year 2015 (Yin et al., 2017; Schürholz et al., 2020). Besides, pollutants can affect humans indirectly, for instance, pollutants pervade agricultural food products (Ercilla-Montserrat et al., 2018) or disturb livelihood and welfare in cities (Schürholz et al., 2020). The exhaust gas is generated by huge amounts of cars and industries by the development of industrialisation, which increases air pollution highly (Chen et al., 2021). Generally, the air is influenced using various features (Zheng et al., 2013, 2015; Carbajal-Hernández et al., 2012), namely illumination and temperature. In addition, these factors may manipulate each other or produce physical and chemical reactions; therefore air quality prediction is more complex, dynamic and variable. However, air pollution management is more difficult, and it cannot be completely resolved in the least period.

In modern days, the impact of particulate matter (PM) on human fitness becomes a modern research area (Jadhav and Arunkumar, 2018). Meanwhile, PM is a composite assortment of small particles as well as fluid droplets, which contract into the air. The PM can go through the respiratory system from medical concepts. These particles may affect the lungs and heart and they generate serious health issues due to the breath in polluted air. Moreover, long-term experience with high concentrations of atmospheric PM can generate reduced lung operation and early death (Turner et al., 2011; Lin et al., 2020). PM_{2.5}, which is a PM with a diameter minimum of 2.5 μm is a significant index to measure and control air pollution degree, which has considerable interest in modern days (Zhang et al., 2021). Furthermore, meteorological aspects have a great influence on the accretion of PM₁₀. The meteorological elements can control the alternations in atmospheric PM₁₀ concentration in various areas (Amodio et al., 2012; Lin et al., 2020). Various studies are performed in the Swiss area, which exhibits that the concentration of PM₁₀ is associated with wind speed, atmospheric temperature, and surface radiation and it is connected to sulphur dioxide (SO₂), total suspended particles (TSP) and nitrogen dioxide (NO₂) of local pollution emissions (Monn et al., 1995; Lin et al., 2020). The weighted fuzzy inference model was developed in Olvera-García et al. (2016) for air quality prediction, although new rules based on parameter behaviours were not included for better computational performance. The PM₁₀ concentration in Taiwan is affected based on several meteorological elements, such as temperature, relative humidity, carbon monoxide (CO), NO₂, ozone (O₃), and SO₃ and wind speed (Lin et al., 2020). The impact of every meteorological factor is different under dissimilar seasonal situations. Additionally, air quality prediction can assist humans to make preventive care in everyday life and generate improved arrangements. However, air quality prediction is still a major challenge owing to the coupling between various elements in the prediction process (Leksmono et al., 2006; Lin et al., 2020).

Air quality data has extensive trouble worldwide. Moreover, time series data identification approaches, such as time series prediction models (Benhaddi and Ouarzazi, 2021), and traditional machine learning methods (Li et al., 2019) are frequently employed for air quality detection. Additionally, forecast approaches using the deep learning model (Zhang al., 2021) extract the features from air quality data and obtain better recognition accuracy. The standard machine learning approaches, like principal component analysis (PCA), back propagation (BP) network, regression analysis and artificial neural network (ANN) are considered for air quality prediction (Chen et al., 2021). Besides, the major

intention of the air quality prediction process is to identify pollutant concentration based on future-based meteorological, historical air quality data, etc. (Li et al., 2016; Zhou et al., 2014). Moreover, the previous studies that can predict air pollutant concentrations mainly include two types, namely deterministic and statistical techniques. Recently, various advanced artificial intelligence (AI) techniques are employed for establishing nonlinear relationships as well as extracting difficult features in several remote sensing and geosciences applications, like remote image classification (Yan et al., 2019), spatial data mining, and unmixing for hyperspectral imagery and so on. In addition, random forest (RF), support vector machine (SVM), and ANN techniques are extensively utilised for air quality prediction and they obtained improved performance than conventional statistical algorithms (Zhang et al., 2021).

The major purpose of this research is to devise and introduce an air quality prediction technique, named PRCSO-based DRNN.

The major contribution of this research is explicated below:

- Developed PRCSO-based DRNN technique for air quality and carbon monoxide prediction: the DRNN model is utilised for predicting the quality of air as well as carbon monoxide. In addition, DRNN is trained by a developed PRCSO algorithm based on every location separately. The developed PRCSO technique is devised by integrating CSO, PO algorithm and ROA.

2 Literature survey

Schürholz et al. (2020) devised long short term memory-based neural network (LSTM-NN) for air quality calculation. This model has three phases, namely context modelling, situation reasoning, and prediction. Here, context space theory (CST) was employed for modelling context. Moreover, a deep learning scheme was applied for identifying air quality. This model obtained enhanced precision with minimal error, although effectual data was not included for avoiding several issues, like potential disturbance and measuring breakdown station. Zhang et al. (2021) introduced empirical mode decomposition (EMD) and bidirectional (BiLSTM) driven NN for predicting the quality of air. In addition, EMD was employed along with an unsupervised transferring approach to extract important features. This model obtained enhanced accuracy and scalability, although the error rate was high. Mao et al. (2021) modelled deep learning technique for the prediction of air quality. The temporal sliding LSTM extended (TS-LSTME) algorithm enabled NN for air quality prediction. Furthermore, optimum time lag spatiotemporal correlation was included to realise sliding prediction, which enhances the performance of prediction. This technique attained an improved correlation coefficient in large time series data but still failed to decrease computational complicity. Ma et al. (2019) presented transferred bi-directional (TL-BLSTM) model for air quality prediction. Originally, input data was attained and it was pre-processed using time lag determination and time series modelling. In addition, the BLSTM model was trained to identify air quality. Moreover, a transfer learning model was included for improving the precision of air quality prediction. This approach obtained improved prediction accuracy, however not reduced the computational complexity.

Table 1 Literature survey

<i>Authors</i>	<i>Methods</i>	<i>Advantages</i>	<i>Disadvantages</i>
Schürholz et al. (2021)	Long short-term memory-based neural network (LSTM-NN) for air quality calculation.	This model obtained enhanced precision with minimal error.	Effectual data was not included for avoiding several issues, like potential disturbance and measuring breakdown station
Zhang et al. (2021)	Empirical mode decomposition (EMD) and bidirectional (BiLSTM) driven NN for predicting quality of air.	This model obtained enhanced accuracy and scalability.	The error rate was high.
Mao et al. (2021)	Deep learning technique for prediction of air quality.	This technique attained an improved correlation coefficient in large time series data.	Failed to decrease computational complicity.
Ma et al. (2019)	Transferred bi-directional (TL-BLSTM) model for air quality prediction.	This approach obtained improved prediction accuracy.	Not reduce the computational complexity.
Lin et al. (2020)	Neuro-fuzzy modelling scheme for air quality prediction.	The processing time of this technique was minimal.	Multi-step ahead prediction was not performed well in reducing accumulation errors.
Chen et al. (2021)	Integrated dual LSTM for air quality prediction.	The computational error was highly decreased.	Small probabilities were created in the results.
Jin et al. (2020)	Deep hybrid technique for air quality identification.	The prediction accuracy was highly increased.	Failed to reduce computational complexity.
Espinosa et al. (2021)	Time series forecasting-based multi-criteria model for air quality forecast.	The computational error was less in this approach.	Failed to compute step-ahead prediction for better performance.

Lin et al. (2020) introduced a neuro-fuzzy modelling scheme for air quality prediction. In this model, training data was divided into fuzzy clusters, whose membership functions were classified by computed variance and mean values. Additionally, fuzzy rules were extracted as well a four-layer fuzzy NN was formulated from fuzzy clusters. Furthermore, descent backpropagation, and particle swarm optimisation (PSO) approaches were employed for training the NN. The processing time of this technique was minimal, even though multi-step ahead prediction was not performed well for reducing accumulation errors. Chen et al. (2021) developed integrated dual LSTM for air quality prediction. Here, the sequence to sequence (Seq2Seq) model was applied for establishing single-factor prediction. Afterwards, LSTM was utilised with an attention scheme to perform multi-factor prediction. At last, the eXtreme gradient boosting (XGBoosting) scheme was utilised for incorporating LSTM and Seq2Seq techniques. The computational error was highly decreased, but still, small probabilities were created in the results. Jin et al. (2020) designed a deep hybrid technique for air quality identification. In this model, convolutional neural network (CNN) and EMD were applied for categorising a fixed

amount of groups using frequency features. Afterwards, gated recurrent unit (GRU) was trained for each set as sub prediction. The prediction accuracy was highly increased, although failed to reduce computational complexity. Espinosa et al. (2021) presented time series forecasting-based multi-criteria model for air quality forecast. In this model, statistical tests as well as a multi-criteria optimisation approach were designed to select the best representation of the prediction scheme. The computational error was less in this approach; however, this model failed to compute step-ahead prediction for better performance. Table 1 displays the literature survey of the existing methods and the proposed method.

3 Proposed PRCISO approach for air quality and carbon monoxide prediction

This section elucidates about developed PRCISO-based deep learning algorithm for air quality and carbon monoxide prediction. Air quality prediction is an essential process in town regions because it causes serious health issues for humans. This developed air quality prediction process mainly contains three sections, including pre-processing, technical indicators, and prediction process. The time series air quality data is considered as input from a database, and this data is based on various locations, like Delhi, Chennai, Ahmadabad and so on. Afterwards, pre-processing is performed based on missing value imputation for removing the redundant value. Furthermore, technical indicators and location information are extracted for further prediction processes. At last, carbon monoxide and air quality prediction is carried out using DRNN, and it is trained by a developed optimisation algorithm, termed the PRCISO scheme. The block diagram of the developed PRCISO technique for air quality and carbon monoxide prediction is exposed in Figure 1.

3.1 Input data

The developed air quality and carbon monoxide prediction is performed using the time series data. Let us assume the time series data D with various attributes, and it is expressed as:

$$C = \{c_q\}; (1 \leq q \leq I) \quad (1)$$

where C is a dataset, I implies the total amount of time samples and c_q refers to time series data at q^{th} index. Here, input time series data c_q is considered and it is further passed to the pre-processing process.

3.2 Pre-processing using missing value imputation

The time series data c_q is taken and it is pre-processed by missing value imputation for decreasing the redundant data. In addition, the input raw data is transformed into comprehensible data format in pre-processing process and the prediction accuracy is highly enhanced by this method. The missing value imputation is used for transferring the data to a variety of similar data. Here, missing values are identified using the feature

average in non-missing values finally, missing values are filled. The output of pre-processed data is indicated as U_q .

Figure 1 Block diagram of developed PRCSO algorithm for predicting the air quality (see online version for colours)



3.3 Location and technical indicator extraction

The pre-processed data U_q is considered as input for further location and technical indicator extraction process. Here, several significant technical indicators and location information is extracted for further prediction process and is explained below.

3.3.1 Normalised average true range

Normalised average true value is the estimation of air quality at two different locations, which is calculated by,

$$S_1 = \frac{A}{close} \times 100 \quad (2)$$

where A specifies an average true range and normalised average true range feature is indicated as S_1 .

3.3.2 Triple exponential moving average

TEMA is a type of technical indicator, which affords a moving average with minimal lag. TEMA is calculated by.

$$TEMA = (3 * H_1) - (3 * H_2) + H_3 \quad (3)$$

where H_1 indicates exponential moving average (EMA), H_2 refers to EMA of B_1 , and H_3 implies EMA of B_3 , and EMA is estimated by $H_1 = H(1) + \lambda \times (close - H(1))$ where, $\lambda = 2/(B + 1)$, B represents the smoothing period. The TEMA indicator is signified as S_2 .

3.3.3 Adaptive moving average

Adaptive moving average is another technical indicator, which employs scalable constant in place of fixed constant for smoothing air quality data. The adaptive moving average indicator is denoted as S_3 .

3.3.4 Keltner channels

Generally, the Kelner channel is a volatility-based technical indicator where three lines including the upper band, middle line and lower band are available. The middle line of the Keltner channel is EMA, while the other two bands are placed above and below the EMA. Therefore, Keltner channel equations are illustrated by,

$$X = H_1 \quad (4)$$

$$E_U = H_1 + 2 * A \quad (5)$$

$$E_L = H_1 - 2 * A \quad (6)$$

where A represents an average true range, X implies Keltner channel middle line, E_U is Keltner channel upper band, E_L specifies Keltner channel lower band and H_1 indicates EMA. The Keltner channel indicator is specified as S_4 .

3.3.5 Rate of change

ROC is utilised to estimate the rate of alternation concerning the previous time interval of air quality, which is denoted as:

$$S_5 = \frac{Z(r)}{Z(r-o)} * 100 \quad (7)$$

where Z indicates air quality, $Z(r)$ indicates air quality at period r and $Z(r - o)$ signifies the change of air quality at time r . The ROC indicator is denoted as S_5 .

3.3.6 William %R

William %R is utilised to compute the terminating air quality of the day in recent ten days, which is denoted as:

$$S_6 = \frac{I}{M} * 100 \tag{8}$$

where M denotes the highest lowest air quality, and I denotes the highest closed air quality. Here, William’s %R indicator is denoted as S_6 .

3.3.7 Simple moving average

SMA is an effective technical indicator, and it is measured as the average air quality rate for a particular period, which is denoted by,

$$S_7 = \frac{1}{p} \sum_{\delta=0}^{p-1} O_{y-\delta} \tag{9}$$

where p refers to input window length, O_y implies close air quality for time y , and S_7 refers to SMA technical indicator.

3.3.8 Relative strength index

RSI exhibits weakness of detected air quality by considering the final closing range of air quality, which is expressed in the following equation.

$$S_8 = \frac{avg(T_{up})}{avg(T_{up}) + avg(T_{down})} * 100 \tag{10}$$

$$T_{up} = 1 * (T(r) - T(r - 1)); \text{ if } T(r) - T(r - 1) > 0 \tag{11}$$

$$T_{down} = 1 * (T(r - 1) - T(r)); \text{ if } T(r) - T(r - 1) < 0 \tag{12}$$

where T_{up} the term implies increased air quality, T_{down} denotes decreases air quality, and the RSI indicator is represented as S_8 .

3.3.9 Commodity channel index

CCI is employed for representing variations in air quality and predicting the finishing and beginning values. It ranges from -100 to 100 as well as values outside the range signify the highly polluted and less polluted circumstances, which is indicated in the below equation.

$$S_9 = \frac{H_{ip} - H_{atp}}{0.015 * P} \tag{13}$$

where P refers to mean deviation, H_{ap} denotes average typical pollution range, H_p specifies typical pollution range, which is given by,

$$H_p = \frac{H_{close} + H_{lw(d)} + H_{hg(d)}}{3} \quad (14)$$

The CCI technical indicator is represented as S_9 .

3.3.10 Stochastic %K

This technical indicator is used for estimating the maximum and minimum value of the air quality range for previous days.

$$S_{10} = 100 * \frac{(N - Y)}{(L - Y)} \quad (15)$$

where Y indicates lowest air quality range, L signifies highest air quality range and the Stochastic % K indicator is denoted as S_{10} .

3.3.11 Aroon Indicator

Aroon indicator is utilised for finding the air quality range variations with regards to time, which is estimated by the following expression,

$$S_{11} = W_{up} - W_{down} \quad (16)$$

$$W_{up} = 100 \times \frac{25 - v_{25}}{25} \quad (17)$$

$$W_{down} = 100 \times \frac{25 - \bar{v}_{25}}{25} \quad (18)$$

where v_{25} refers to high data since 25 days period, and \bar{v}_{25} signifies low data since 25 days period, and the Aroon indicator is indicated as S_{11} .

3.3.12 Average directional movement index

ADMI defines air quality strength, and it identified the previous ten days as equivalent to the input window length. This indicator specifies less air quality and high air quality situations in specific locations at particular time.

$$S_{12} = 100 * \frac{G^+ - G^-}{G^+ + G^-} \quad (19)$$

The ADMI technical indicator is denoted as S_{12} .

Therefore, the total technical indicators extracted from pre-processed time series data U_q is specified as:

$$S = \{S_q\}; q \in \{1, 2, \dots, 12\} \quad (20)$$

where S specifies total extracted indicators, which are further subjected to the prediction process.

The location information is obtained by the difference between the location of the testing place and its trained nearby place, which is given by,

$$V_q = \|N_{loc}^P - M_{loc}^P\| \tag{21}$$

where V_q implies extracted location information, N_{loc}^P indicates the nearest location that is, the neighbouring place of the test location and M_{loc}^P refers location of the place selected for air quality prediction. For example, if the model is trained for Assam, Ahmadabad, and Delhi and the prediction is to be made for Gujarat, then the location of nearby places to Gujarat will be taken for the difference.

3.4 Air quality and carbon monoxide prediction using developed PRCISO-based DRNN

Once the imperative technical indicators and location information is extracted, then air quality prediction and carbon monoxide prediction are done. The extracted technical indicators S as well as location information V_q is taken for predicting air quality and carbon monoxide prediction using DRNN. In addition, the DRNN (Inoue et al., 2018) is trained by an introduced optimisation technique, named the PRCISO approach. The devised PRCISO model is newly devised by integrating ROA, CSO, and PO.

3.4.1 Structure of DRNN

The DRNN classifier is applied for predicting air quality and carbon monoxide prediction using the extracted technical indicators and location information. The DRNN classifier effectively increases the recognition rate with less processing duration, thus it is used for air quality and carbon monoxide prediction processes. The DRNN model is an ANN that records dynamic time series by directed connecting of nodes at the hidden layer and has a large number of hidden layer results. This structure differs from a feed-forward network in that it uses feed-forward and feedback connections between internal processing modules to record input sequences at various time states. As a result of the DRNN classifier's more reliable transformation of the technical data, its capacity for prediction is increased. Regarding time, this network largely consisted of several nonlinear layers. Additionally, the entirety of the sequence's data is effectively analysed, and the present output is used to forecast the value of the subsequent output. This model made use of historical data over a small number of phases and information in random order. Additionally, it converts the input series into a hidden state sequence before using the hidden state to convert the input series into output series using a feature learning model. Let us assume input is subjected to the input layer at a time g as R_g and hidden layer state at time g as Q_g . The hidden layer process is expressed as,

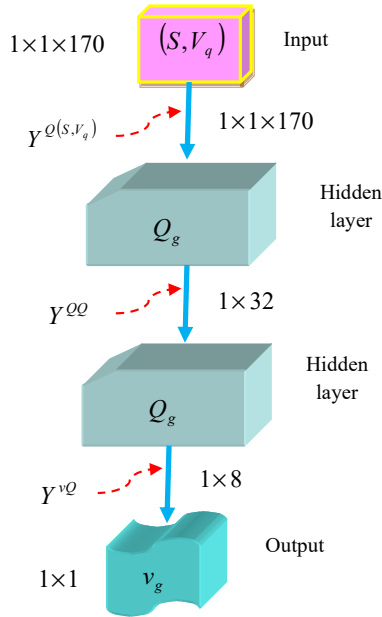
$$Q_g = h((S, V_q)Y^{Q(S,V_q)} + Q_{g-1}Y^{QQ}) \tag{22}$$

where h signifies the nonlinear function, such as tanh and ReLU functions, Q_{g-1} denotes the previous hidden layer state, Y indicates weight factor, $Y^{Q(S,V_q)}$ expresses weight among input and hidden layer, Y^{QQ} denotes weight amongst hidden layers, and (S, V_q) symbolises input. The output estimated at the output layer is specified as,

$$v_g = h(Q_g Y^{vQ}) \tag{23}$$

where v_g represents output, h symbolises function, Y^{vQ} refers to weight among hidden and output layers. Meanwhile, the optimal weight value is estimated by devised PRCSO approach using a training process. Figure 2 shows the structural diagram of the DRNN classifier.

Figure 2 Structural diagram of DRNN classifier (see online version for colours)



3.4.2 Proposed PRCSO for the training process of DRNN

Additionally, the DRNN classifier is trained by a developed PRCSO algorithm for obtaining better prediction performance. Besides, the training process is carried out based on every location individually. The developed PRCSO approach is newly designed by incorporating ROA (Binu and Kariyappa, 2018), CSO (Cheng and Jin, 2014), along with PO (Askari et al., 2020). By promoting rider groups, an optimisation process known as the ROA is produced. Assailants bypass riders, follows, and overtaker riders are among the four categories of motorcyclists included in ROA. Another more effective method is ROA, which uses a fictitious computational process to handle various optimisation problems. Additionally, the PSO method is stimulated in the design of the CSO procedure. This plan was created using a straightforward technique that mimics social animal behaviours, such flocking of birds. On the other hand, PO was created by drawing inspiration from the multi-phased political process. The strategy is broken down into five stages: party formation and constituency distribution, party switching, election administration, parliamentary activities, and inter-party selection. While other stages function in a loop, the party generation and constituency allocation stage operates initially. Additionally, the PO framework supported both the exploration and exploitation

phases. The CSO technique is incorporated into PO to shorten the processing time because PO has a higher temporal complexity. The scalability of high-dimensional issues was significantly improved by the CSO method. The algorithmic process of developed PRCO technique is explicated below,

- 1 Initialisation: at first, rider parameters are initiated randomly, which is expressed as:

$$G_k = \{G_k(a, b)\}; 1 \leq a \leq X, 1 \leq b \leq Z \tag{24}$$

where X – +refers quantity of riders, Z indicates the dimension of coordinates, $G_k(a, b)$ denotes the position of a^{th} rider at the moment b . Once the group initialisation is finished, then rider parameters are initialised. The rider parameters including brake S_w , steering K_w , gear T_w , and accelerator B_w are initialised. Here, $G \in Y, Q$.

- 2 Computation of fitness function: the fitness measure is estimated using the difference between final target output and classified output. The solution with the least error is taken as the best optimal solution, and the fitness function is calculated by the following expression.

$$\vartheta = \frac{1}{j} \sum_{o=1}^j (v_g^* - v_g) \tag{25}$$

where ϑ implies fitness function, j signifies total amount of training samples, v_g^* indicates target output and v_g refers to DRNN classifier.

- 3 Identification of leading rider: the top rider is projected using the fitness measure value that was calculated. The cyclist chosen as the leader is the one with the highest fitness value, and the position of the leading rider is regularly adjusted based on fitness value.
- 4 Update the location of the rider: by updating the riders’ positions at the moment in time, the leading rider is determined. Here is an explanation of where each rider in a group is located:

- Update bypass rider position

In most cases, bypass riders avoid the well-travelled way without taking their leading path into account. As a result, the phrase below updates the location of the bypass rider.

$$G_{k+1}^b(a, b) = \eta [G_k(\varphi, b) * \varpi(b) + G_k(\varepsilon, b) * (1 - \varpi(b))] \tag{26}$$

where η indicates random integer from 0 and 1, φ specifies random integer, which ranges from 0 to X , ϖ represents a random number from 0 to 1 with dimension of $1 \times Z$, ε implies an integer value with 1 and X . Therefore, all riders present in the bypass set update their location to become a winner.

- Update the position of the follower

The follower speedily attains the target by updating the location through the position of the leading rider. The follower location is updated based on the chosen values of Z , since the follower’s location is based on the coordinate selector. The location of the follower is updated by the below equation.

$$G_{k+1}^f(a, f) = G^F(F, f) + \left[\cos(A_{a,f}^i) * G^F(F, f) * c_a^i \right] \quad (27)$$

where f represents coordinate selector, G^F specifies the location of leading rider, F denotes leading rider, $A_{a,f}^i$ implies steering angle of a^{th} rider in f^{th} coordinate, and c_a^i is the distance travelled by a^{th} rider.

- Update the position of the overtaker

The direction indication, relative success rate, and coordinate selector are the three features that are typically used to update the overtaker. The overtaker's position-updated expression is written as,

$$G_{k+1}^o(a, f) = \left(\frac{E_2 + \delta E_3 - 1}{E_2 + \delta E_3} \right) \left[A_i^n(a) * G^F(F, f) - \frac{E_1 M_i(a, f) + E_2 M_i(s, f) + \delta E_3 \bar{M}_y}{1 - E_2 - \delta E_3} \right] \quad (28)$$

where $E_1, E_2, E_3 \in [0, 1]$, \bar{M}_y indicates mean position value, δ signifies random integer, $M_i(a, f)$ is the position of a^{th} rider at f^{th} coordinate, $M_i(s, f)$ is the position of s^{th} rider at f^{th} coordinate.

$$A_i^n(a) = \left[\frac{2}{1 - \log(N_i^T(a))} \right] - 1 \quad (29)$$

$$N_i^T(a) = \frac{s_i(a)}{\max_{a=1}^E s_i(a)} \quad (30)$$

Here, $N_i^T(a)$ specifies the relative success rate of a^{th} rider at a time i and $s_i(a)$ represents the success rate of a^{th} rider at a time i .

$$G_{k+1}^o(a, f) = \left(\frac{E_2 + \delta E_3 - 1}{E_2 + \delta E_3} \right) A_i^n(a) * G^F(F, f) - \left(\frac{E_2 + \delta E_3 - 1}{E_2 + \delta E_3} \right) \frac{E_1 M_i(a, f) + E_2 M_i(s, f) + \delta E_3 \bar{M}_y}{1 - E_2 - \delta E_3} \quad (31)$$

From PO,

$$G_{k+1}^o(a, f) = x^* + (2c + 1) |x^* - G_k(a, f)| \quad (32)$$

Let us assume $x^* > G_k(a, f)$,

$$G_{k+1}^o(a, f) = x^* + (2c + 1)(x^* - G_k(a, f)) \quad (33)$$

$$G_{k+1}^o(a, f) = x^*(1 + 2c - 1) - (2c - 1)G_k(a, f) \quad (34)$$

$$G_{k+1}^o(a, f) = 2cx^* - (2c - 1)G_k(a, f) \quad (35)$$

$$2cx^* = G_{k+1}^o(a, f) + (2c - 1)G_k(a, f) \quad (36)$$

$$x^* = \frac{G_{k+1}^o(a, f) + (2c - 1)G_k(a, f)}{2c} \quad (37)$$

In order to obtain better performance, the updated PO is included in the leading rider's location of ROA. Substitute equation (37) in the leading rider's position of equation (31),

$$G_{k+1}^o(a, f) = \left(\frac{E_2 + \delta E_3 - 1}{E_2 + \delta E_3} \right) A_i^n(a) * \frac{G_{k+1}^o(a, f) + (2c-1)G_k(a, f)}{2c} - \left(\frac{E_2 + \delta E_3 - 1}{E_2 + \delta E_3} \right) \frac{E_1 M_i(a, f) + E_2 M_i(s, f) + \delta E_3 \bar{M}_y}{1 - E_2 - \delta E_3} \quad (38)$$

$$G_{k+1}^o(a, f) = \left(\frac{E_2 + \delta E_3 - 1}{E_2 + \delta E_3} \right) A_i^n(a) * \frac{G_{k+1}^o(a, f)}{2c} + \left(\frac{E_2 + \delta E_3 - 1}{E_2 + \delta E_3} \right) * A_i^n(a) \frac{(2c-1)}{2c} G_k(a, f) - \left(\frac{E_2 + \delta E_3 - 1}{E_2 + \delta E_3} \right) * \frac{E_1 M_i(a, f) + E_2 M_i(s, f) + \delta E_3 \bar{M}_y}{1 - E_2 - \delta E_3} \quad (39)$$

$$G_{k+1}^o(a, f) - \left(\frac{E_2 + \delta E_3 - 1}{E_2 + \delta E_3} \right) A_i^n(a) * \frac{G_{k+1}^o(a, f)}{2c} = \left(\frac{E_2 + \delta E_3 - 1}{E_2 + \delta E_3} \right) * A_i^n(a) \frac{(2c-1)}{2c} G_k(a, f) - \left(\frac{E_2 + \delta E_3 - 1}{E_2 + \delta E_3} \right) * \frac{E_1 M_i(a, f) + E_2 M_i(s, f) + \delta E_3 \bar{M}_y}{1 - E_2 - \delta E_3} \quad (40)$$

$$G_{k+1}^o(a, f) \left(1 - \left(\frac{E_2 + \delta E_3 - 1}{E_2 + \delta E_3} \right) * \frac{A_i^n(a)}{2c} \right) = \left(\frac{E_2 + \delta E_3 - 1}{E_2 + \delta E_3} \right) * A_i^n(a) \frac{(2c-1)}{2c} G_k(a, f) - \left(\frac{E_2 + \delta E_3 - 1}{E_2 + \delta E_3} \right) * \frac{E_1 M_i(a, f) + E_2 M_i(s, f) + \delta E_3 \bar{M}_y}{1 - E_2 - \delta E_3} \quad (41)$$

$$G_{k+1}^o(a, f) = \left[1 - \left(\frac{E_2 + \delta E_3 - 1}{E_2 + \delta E_3} \right) * \frac{A_i^n(a)}{2c} \right]^{-1} * \left(\frac{E_2 + \delta E_3 - 1}{E_2 + \delta E_3} \right) * A_i^n(a) \frac{(2c-1)}{2c} G_k(a, f) - \left(\frac{E_2 + \delta E_3 - 1}{E_2 + \delta E_3} \right) * \frac{E_1 M_i(a, f) + E_2 M_i(s, f) + \delta E_3 \bar{M}_y}{1 - E_2 - \delta E_3} \quad (42)$$

where c signifies random integer, which lies from $[0, 1]$.

- Update the position of an attacker

The leader's position is connected to the attacker's because the attacker wants to steal the leader's location. Additionally, the following equation is used to update the attacker's location:

$$G_{k+1}^s(a, b) = G^F(F, b) + [\cos(A_{a,f}^i) * G^F(F, b)] + c_a^i \quad (43)$$

where G^F specifies the location of the leading rider, F denotes leading rider, $A_{a,f}^i$ signifies the steering angle of a^{th} rider in f^{th} coordinate and c_a^i is distance travelled by a^{th} rider.

- 5 Check feasibility of solution: following the conclusion of rider position identification, the rider with the best fitness score is selected as the best option.
- 6 Updation of rider parameter: the rider parameters are approximated in order to determine the optimal solution, while the activity counter is computed to update many parameters, including steering angle and gear.
- 7 Termination: the iteration is continual until the identification of the leading rider is obtained. Here, the leading rider position of the RCSO algorithm is integrated with PO, thus the quality of the air prediction approach is highly improved. Moreover, the DRNN classifier significantly enhanced the performance of air quality prediction with less duration. In addition, the training process of DRNN is done by the developed PRCO technique, which obtained better prediction performance in real-time.

4 Results and discussion

This section deliberates the evaluation of the developed PRCO-based DRNN for air pollutant quality and carbon monoxide prediction.

4.1 Experimental setup

The execution of devised PRCO-based DRNN is done using the PYTHON tool. Table 2 shows the experimental parameters of the developed system.

Table 2 Experimental parameters

<i>Parameters</i>	<i>Values</i>
Iteration	100
Epochs	100
Loss	'mean_squared_error'
Batch size	32
Population	10
Learning rate	0.1
Lower bound	0
Upper bound	1

4.2 Dataset description

The introduced air pollutant quality and carbon monoxide prediction is executed using Air quality data in the India dataset (India Air Quality Dataset, https://www.kaggle.com/shrutibhargava94/india-air-quality-data#_sid=js0). This data generally comprises air quality data as well as air quality index (AQI) at hourly and everyday levels from different locations across dissimilar cities in India. The air quality data mainly includes five files including city_hour, station_hour, station_day, city_day, and stations. Here, three cities, such as Chennai (City-1), Delhi (City-2) and Kolkata (City-3) are considered for the developed prediction process.

4.3 Performance metrics

The performance of the designed PRCSO-based DRNN is evaluated based on several metrics including mean square error (MSE), and mean absolute percentage error (MAPE) and it is explained as follows.

1 Mean square error

MSE is defined as the total squared error between the actual and anticipated value, and equation (25) gives its expression.

2 Mean absolute percentage error

Generally, MAPE is calculated by average absolute percentage error in all periods minus the predicted value divided by its actual value.

$$\psi = \frac{1}{u} \sum_{\beta=1}^u \left| \frac{E - E_o}{E} \right| \tag{44}$$

where ψ implies MAPE, u specifies total data, E denotes actual value and E_o represents predicted output.

4.4 Comparative methods

The existing air quality prediction techniques, deep learning (Ma et al., 2019), bidirectional LSTM (Zhang et al., 2021), weighted fuzzy method (Olvera-García et al., 2016), and RCSO-based rider deep LSTM are utilised for comparison of developed air pollutant quality and carbon monoxide approach.

4.5 Comparative analysis

This section specifies a comparative evaluation of the PRCSO-based DRNN for carbon monoxide and air quality prediction for city-1, 2 and 3.

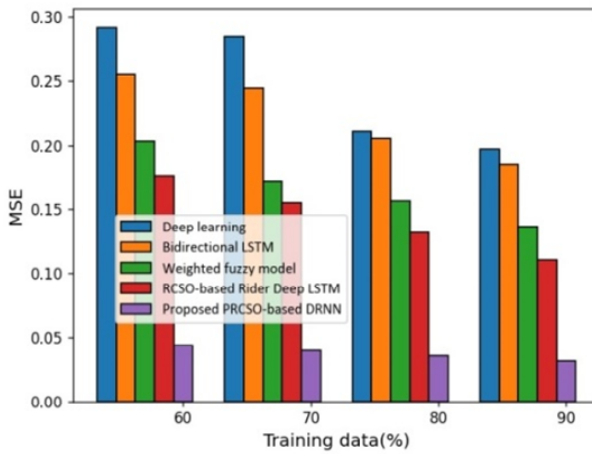
4.5.1 Comparative analysis for carbon monoxide prediction

The comparative evaluation of the PRCSO-based DRNN with carbon monoxide prediction for city-1, 2 and 3 using MSE and MAPE is explicated in this section.

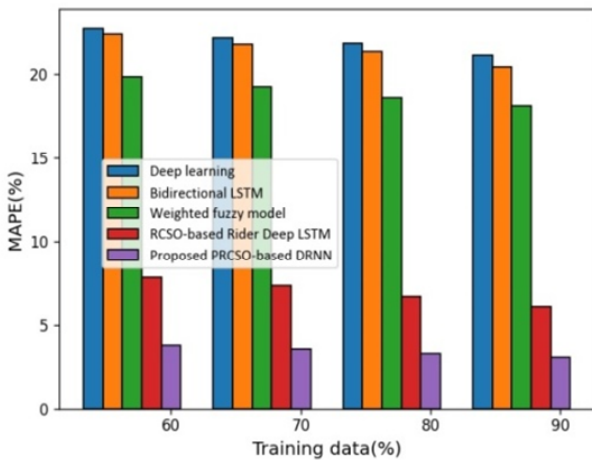
4.5.1.1 Analysis for city-1

By changing the training data percentage, Figure 3 illustrates a comparative evaluation of the city-1 PRCO-based DRNN. A comparison of MSE by adjusting the percentage of training data is shown in Figure 3(a). When compared to existing methods, such as deep learning, bidirectional LSTM, weighted fuzzy method, and RCSO-based rider deep LSTM, which account for 80% of training data, have MSEs of 0.2109, 0.2053, 0.1563, and 0.1316. The MSE of the proposed PRCO-based DRNN is 0.0356. Figure 3(b) shows the MAPE comparison analysis. When the training data percentage is 80, the PRCO-based DRNN is 3.33%, the weighted fuzzy scheme is 18.62%, the bidirectional LSTM is 21.36%, the MAPE of deep learning is 21.88%, the RCSO-based rider deep LSTM is 6.72%.

Figure 3 Comparative analysis of introduced PRCO-based DRNN for city-1, (a) MSE, (b) MAPE (see online version for colours)



(a)

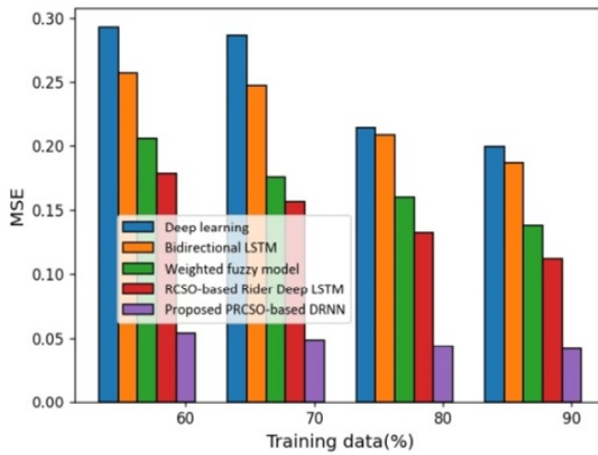


(b)

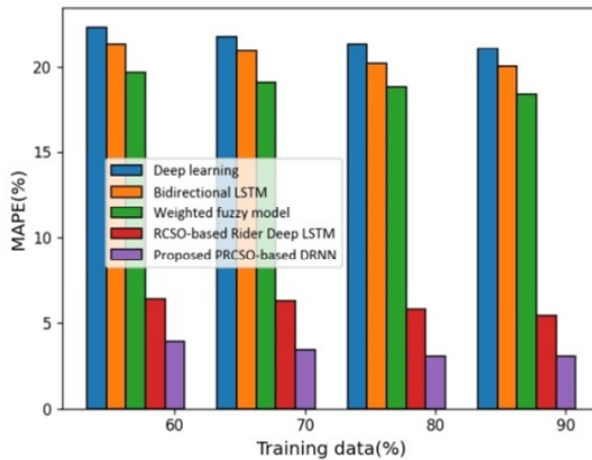
4.5.1.2 Analysis for city-2

The comparative evaluation of the PRCISO-based DRNN for city-2 is represented in Figure 4. Figure 4(a) specifies a comparative analysis of MSE by changing training data %. The MSE of deep learning is 0.2139, bidirectional LSTM is 0.2088, the weighted fuzzy method is 0.1599, RCSO-based rider deep LSTM is 0.1325 and PRCISO-based DRNN is 0.0433, while training data is 80%. Figure 4(b) shows the comparative evaluation of MAPE by changing training data %. The MAPE of developed PRCISO-based DRNN is 3.11%, while existing methods, such as deep learning, bidirectional LSTM, weighted fuzzy method, and RCSO-based rider deep LSTM is 21.35%, 20.20%, 18.83%, and 5.81% for 80% of training data.

Figure 4 Comparative analysis of devised PRCISO-based DRNN for city-2, (a) MSE, (b) MAPE (see online version for colours)



(a)

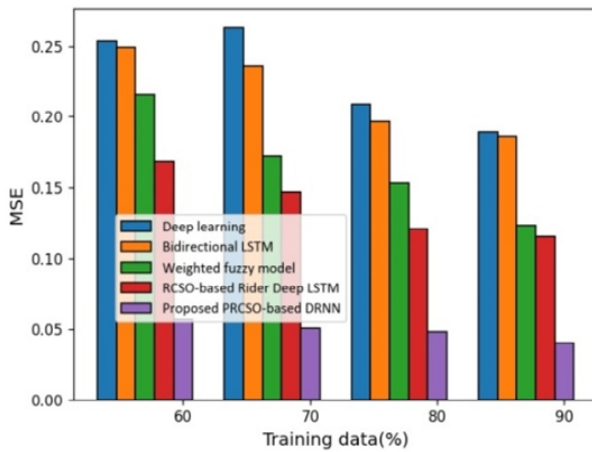


(b)

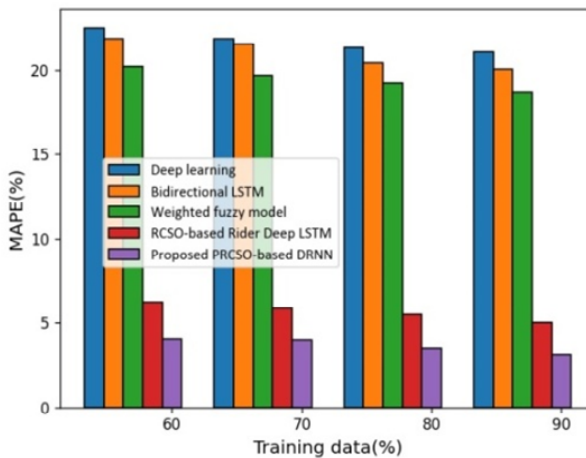
4.5.1.3 Analysis for city-3

By changing the training data percentage, Figure 5 shows the comparative analysis of the PRCSO-based DRNN that was introduced for city-3. The comparison study of MSE by changing training data % is shown in Figure 5(a). While existing techniques like deep learning, bidirectional LSTM, weighted fuzzy method, and RCSO-based rider deep LSTM have MSEs of 0.2086, 0.1966, 0.1527, and 0.121 for 80% of training data, the MSE of the created PRCSO-based DRNN is 0.0486. Figure 5(b) shows the comparative study of MAPE using various training data percentages. When the training data percentage is 80, MAPE of deep learning is 21.33%, bidirectional LSTM is 20.45%, weighted fuzzy scheme is 19.27%, RCSO-based rider deep LSTM is 5.44% and developed PRCSO-based DRNN is 3.48%.

Figure 5 Comparative analysis of devised PRCSO-based DRNN for city-3, (a) MSE, (b) MAPE (see online version for colours)



(a)

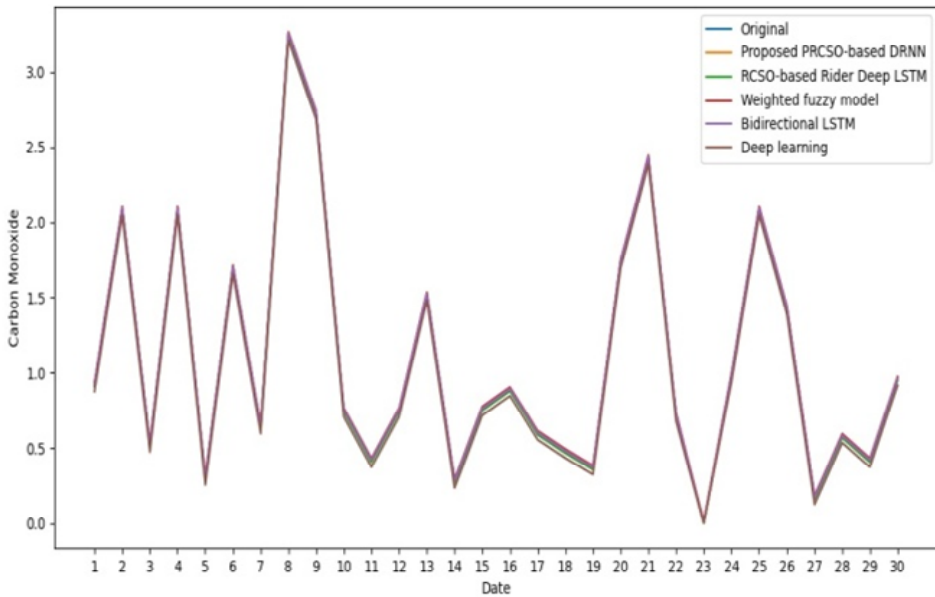


(b)

4.5.1.4 Analysis based on carbon monoxide prediction

Figure 6 explicates the analysis of carbon monoxide with various techniques by varying dates. In date 10, the original value of carbon monoxide is 0.75, whereas the developed PRCSO-based DRNN is 0.7482, RCSO-based DRNN is 0.7376, the weighted fuzzy scheme is 0.7638, bidirectional LSTM is 0.7531, and deep learning technique is 0.7053, such that the error between original carbon monoxide value concerning prediction outputs based on proposed PRCSO-based DRNN, RCSO-based DRNN, weighted fuzzy method, bidirectional LSTM, and deep learning is 0.0017, 0.0123, 0.0138, 0.0138, 0.0031, and 0.0446, respectively.

Figure 6 Analysis for carbon monoxide prediction (see online version for colours)



4.5.2 Comparative analysis for air quality prediction

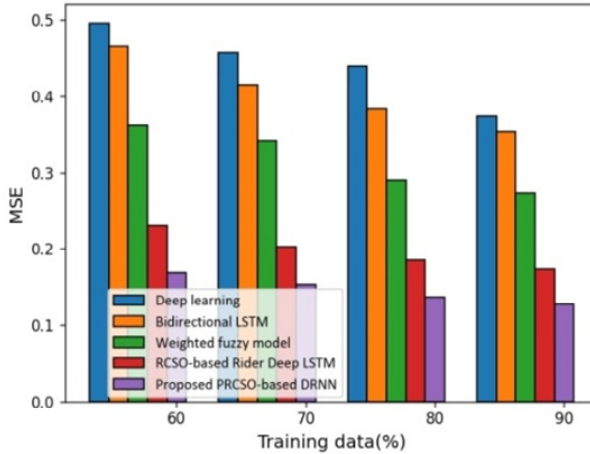
The comparative analysis of devised PRCSO-based DRNN with air quality prediction for city-1, 2 and 3 is explicated in this section.

4.5.2.1 Analysis for city-1

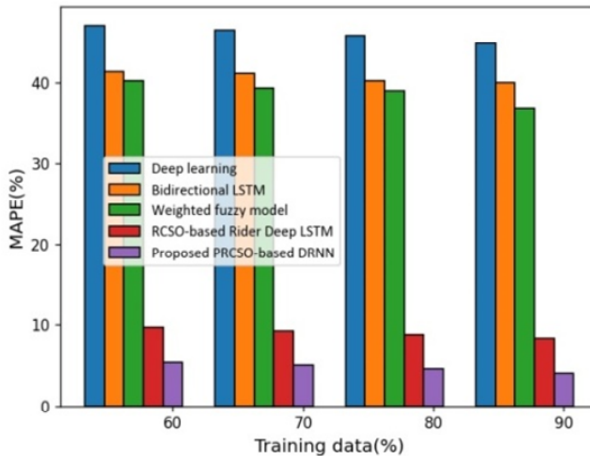
By varying the training data percentage, Figure 7 illustrates the comparative analysis of the generated PRCSO-based DRNN for city-1. The comparison study of MSE using shifting training data percentage is shown in Figure 7(a). The MSE of developed PRCSO-based DRNN is 0.1373, while existing methods, such as deep learning, bidirectional LSTM, weighted fuzzy method, and RCSO-based rider deep LSTM is 0.4396, 0.3835, 0.2910, and 0.1851 for 80% of training data. Figure 7(b) shows the comparative study of MAPE using different training data percentages. When training data percentage is 80, MAPE of deep learning is 45.77%, bidirectional LSTM is 40.18%,

weighted fuzzy scheme is 39.06%, RCSO-based rider deep LSTM is 8.74% and developed PRCSO-based DRNN is 4.55%.

Figure 7 Comparative analysis of introduced PRCSO-based DRNN for city-1, (a) MSE, (b) MAPE (see online version for colours)



(a)



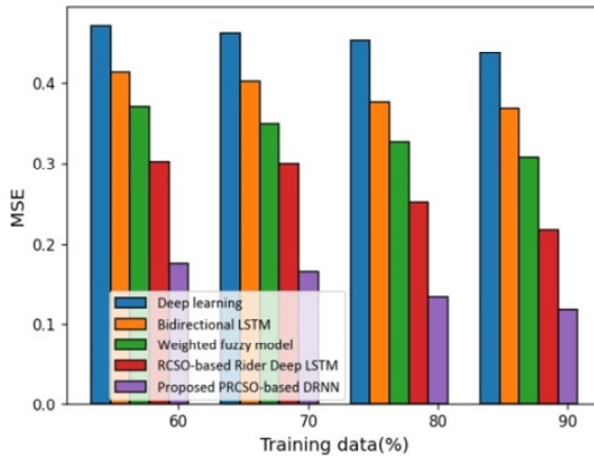
(b)

4.5.2.2 Analysis for city-2

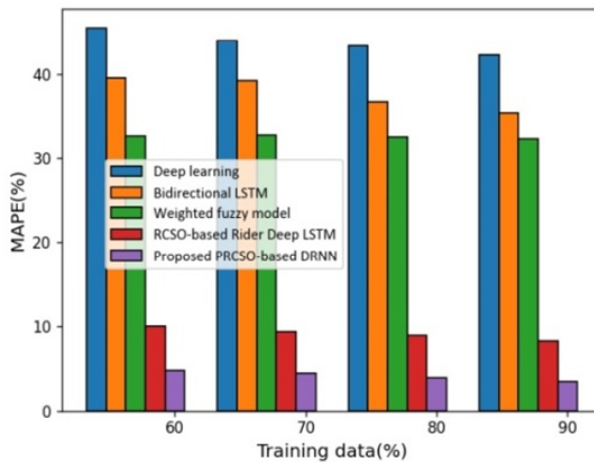
The comparative analysis of developed PRCSO-based DRNN for city-2 by altering training data percentage is represented in Figure 8. Figure 8(a) specifies a comparative analysis of MSE through shifting training data percentage. The MSE of deep learning is 0.4546, bidirectional LSTM is 0.3773, the weighted fuzzy method is 0.3268, RCSO-based rider deep LSTM is 0.2525, and developed PRCSO-based DRNN is 0.1336, while training data is 80%. Figure 8(b) shows the comparative analysis of MAPE through altering training data percentage. The MAPE of developed PRCSO-based DRNN is

3.84%, while existing methods, such as deep learning, bidirectional LSTM, weighted fuzzy method, and RCSO-based rider deep LSTM is 43.33%, 36.69%, 32.64%, and 8.89% for 80% of training data.

Figure 8 Comparative analysis of designed PRCSO-based DRNN for city-2, (a) MSE, (b) MAPE (see online version for colours)



(a)



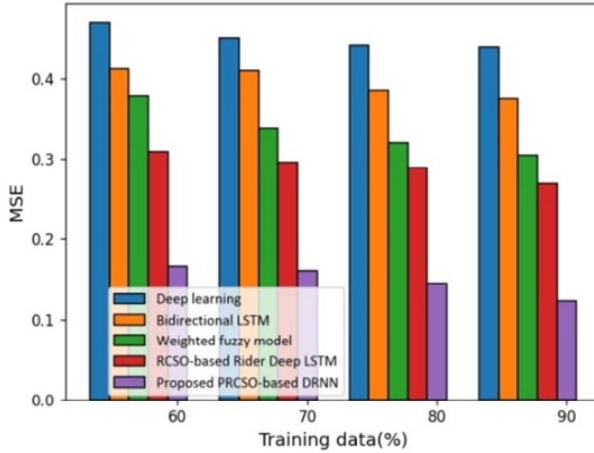
(b)

4.5.2.3 Analysis for city-3

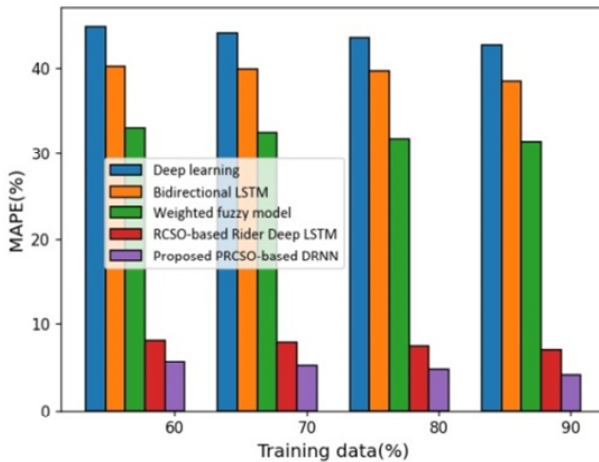
By changing the training data percentage, Figure 9 illustrates the comparative analysis of the generated PRCSO-based DRNN for city-3. Figure 9(a) shows a comparison of MSE by altering the percentage of training data. While current methods like deep learning, Bidirectional LSTM, weighted fuzzy method, and RCSO-based rider deep LSTM have MSEs of 0.4419, 0.3848, 0.3193, and 0.2883 for 80% of training data, the MSE of the

developed PRCSO-based DRNN is 0.1446. Figure 9(b) shows the comparative study of MAPE using different training data percentages. When the training data percentage is 80, MAPE of deep learning is 43.58%, bidirectional LSTM is 39.60%, the weighted fuzzy scheme is 31.68%, RCSO-based rider deep LSTM is 7.52% and developed PRCSO-based DRNN is 4.68%.

Figure 9 Comparative analysis of devised PRCSO-based DRNN for city-3, (a) MSE, (b) MAPE (see online version for colours)



(a)



(b)

4.5.2.4 Analysis based on air quality prediction

Figure 10 explicates the analysis of air quality prediction with various techniques by varying dates. In date 10, the original value of carbon monoxide is 128, whereas the developed PRCSO-based DRNN is 127.99, RCSO-based DRNN is 127.70, the weighted fuzzy scheme is 130.16, bidirectional LSTM is 129.70, and deep learning technique is

133.47, such that the error among original air quality prediction value concerning prediction outputs based on developed PRCO-based DRNN, RCO-based DRNN, weighted fuzzy method, bidirectional LSTM, and deep learning is 0.00363, 0.295, 2.163, 2.163, 1.704, and 5.478, respectively.

Figure 10 Analysis for carbon monoxide prediction (see online version for colours)

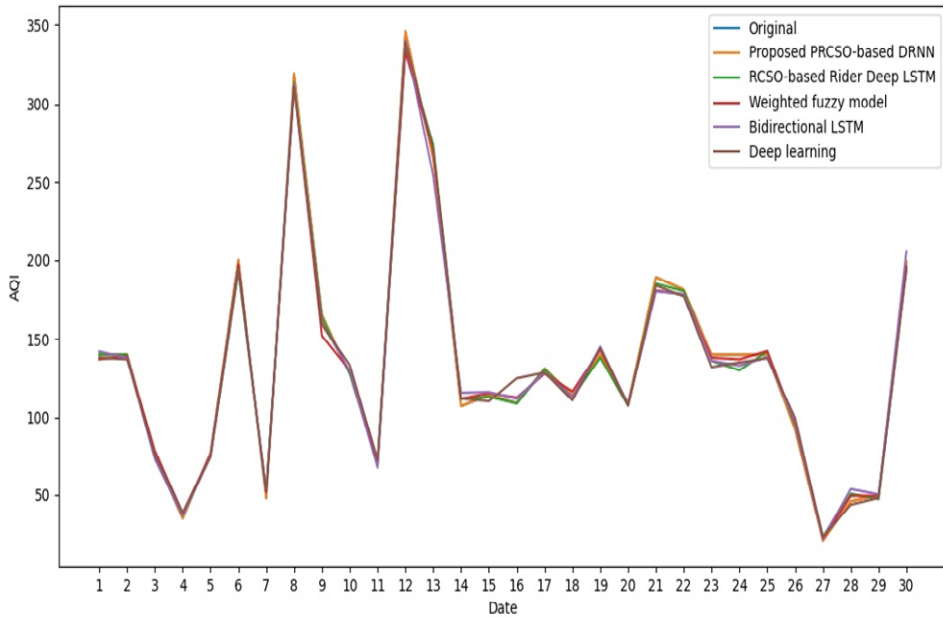


Table 3 Comparative discussion

<i>Based on</i>	<i>For</i>	<i>Metrics</i>	<i>Deep learning</i>	<i>Bidirectional LSTM</i>	<i>Weighted fuzzy model</i>	<i>RCSO-based rider deep LSTM</i>	<i>Proposed PRCO-based DRNN</i>
Carbon monoxide	City-1	MSE	0.1972	0.1854	0.1364	0.1104	0.0313
		MAPE (%)	21.14	20.45	18.07	6.12	3.09
	City-2	MSE	0.1992	0.1872	0.1385	0.1122	0.0411
		MAPE (%)	21.08	20.02	18.37	5.40	3.08
	City-3	MSE	0.1889	0.1861	0.1235	0.1156	0.0400
		MAPE (%)	21.09	20.07	18.76	5.01	3.12
Air quality	City-1	MSE	0.3735	0.3543	0.2743	0.1734	0.1276
		MAPE (%)	44.75	39.97	36.74	8.27	3.99

Table 3 Comparative discussion (continued)

<i>Based on</i>	<i>For</i>	<i>Metrics</i>	<i>Deep learning</i>	<i>Bidirectional LSTM</i>	<i>Weighted fuzzy model</i>	<i>RCSO-based rider deep LSTM</i>	<i>Proposed PRCSO-based DRNN</i>
Air quality	City-2	MSE	0.4385	0.3692	0.3077	0.2176	0.1174
		MAPE (%)	42.32	35.40	32.42	8.27	3.44
	City-3	MSE	0.4398	0.3751	0.3040	0.2688	0.1227
		MAPE (%)	42.70	38.47	31.38	7.11	4.11

4.6 Comparative discussion

In this section, developed PRCSO-based DRNN and existing methods are compared and discussed. Table 3 represents the comparative evaluation in terms of MSE and MAPE with three cities based on carbon monoxide and air quality prediction for 90% of training data. The MSE of developed method is 0.0313, whereas deep learning is 0.1972, bidirectional LSTM is 0.1854, weighted fuzzy scheme is 0.1364, and RCSO-based rider deep LSTM is 0.1104. Similarly, MAPE of deep learning, bidirectional LSTM, weighted fuzzy method, RCSO-based rider deep LSTM, developed PRCSO-based DRNN is 21.14%, 20.45%, 18.07%, 6.12%, and 3.09%.

5 Conclusions

This paper presents the developed air quality prediction approach based on the PRCSO-based DRNN model. Here, time series air quality data is taken from a dataset and it is passed to pre-processing process for eliminating removing redundant data. The missing value imputation model is applied for pre-processing process and pre-processed data is given to the technical extraction process. The location information and the technical indicators are extracted from pre-processed data for the prediction process. The deep learning model, named DRNN is utilised for predicting air quality and carbon monoxide. Moreover, the deep learning technique is trained by a developed optimisation approach, named the PRCSO approach. In addition, the PRCSO algorithm is newly designed by incorporating ROA, CSO as well as PO method. Besides, the training process of DRNN is carried out by the PRCSO model based on every individual location. The performance of the introduced air quality prediction method is evaluated with two metrics, namely MSE and MAPE. The developed PRCSO-based DRNN model obtained better performance with regards to MSE of 0.0313 and MAPE of 3.08%. Here, utilising science and technology, air pollution forecasting aims to identify the types of pollutants that will be present in the atmosphere. In addition, the devised PRCSO-based DRNN technique can be further improved by including another effectual optimisation algorithm with a deep learning technique.

References

- Amodio, M., Andriani, E., De Gennaro, G., Loiotile, A.D., Di Gilio, A. and Placentino, M.C., (2012) ‘An integrated approach to identify the origin of PM 10 exceedances’, *Environmental Science and Pollution Research*, September, Vol. 19, No. 8, pp.3132–3141.
- Askari, Q., Younas, I. and Saeed, M. (2020) ‘Political optimizer: a novel socio-inspired meta-heuristic for global optimization’, *Knowledge-Based Systems*, Vol. 195, p.105709.
- Benhaddi, M. and Ouazazi, J. (2021) ‘Multivariate time series forecasting with dilated residual convolutional neural networks for urban air quality prediction’, *Arabian Journal for Science and Engineering*, April, Vol. 46, No. 4, pp.3423–3442.
- Binu, D. and Kariyappa, B.S. (2018) ‘RideNN: a new rider optimization algorithm-based neural network for fault diagnosis in analog circuits’, *IEEE Transactions on Instrumentation and Measurement*, Vol. 68, No. 1, pp.2–26.
- Carbajal-Hernández, J.J., Sánchez-Fernández, L.P., Carrasco-Ochoa, J.A. and Martínez-Trinidad, J.F. (2012) ‘Assessment and prediction of air quality using fuzzy logic and autoregressive models’, *Atmospheric Environment*, Vol. 60, pp.37–50.
- Chalfen, M. and Kamińska, J.A. (2018) ‘Identification of parameters and verification of an urban traffic flow model, a case study in Wrocław’, in *ITM Web of Conferences*, Vol. 23, p.00005.
- Chen, H., Guan, M. and Li, H. (2021) ‘Air quality prediction based on integrated dual LSTM Model’, *IEEE Access*, June, Vol. 9, pp.93285–93297.
- Cheng, R. and Jin, Y. (2014) ‘A competitive swarm optimizer for large scale optimization’, *IEEE Transactions on Cybernetics*, Vol. 45, No. 2, pp.191–204.
- Ercilla-Montserrat, M., Muñoz, P., Montero, J.I., Gabarrell, X. and Rieradevall, J. (2018) ‘A study on air quality and heavy metals content of urban food produced in a Mediterranean city (Barcelona)’, *Journal of Cleaner Production*, September, Vol. 195, pp.385–395.
- Espinosa, R., Palma, J., Jiménez, F., Kamińska, J., Sciavicco, G. and Lucena-Sánchez, E. (2021) ‘A time series forecasting based multi-criteria methodology for air quality prediction’, *Applied Soft Computing*, December, Vol. 113, p.107850.
- India Air Quality Dataset [online] https://www.kaggle.com/shrutibhargava94/india-air-quality-data#_sid=js0 (accessed 10 November 2021).
- Inoue, M., Inoue, S. and Nishida, T. (2018) ‘Deep recurrent neural network for mobile human activity recognition with high throughput’, *Artificial Life and Robotics*, Vol. 23, No. 2, pp.173–185.
- Jadhav, J.N. and Arunkumar, B. (2018) ‘Web page recommendation system using Laplace correction dependent probability and chronological dragonfly-based clustering’, *International Journal of Engineering and Technology (UAE)*, Vol. 7, No. 3.27, pp.290–302.
- Jin, X.B., Yang, N.X., Wang, X.Y., Bai, Y.T., Su, T.L. and Kong, J.L. (2020) ‘Deep hybrid model based on EMD with classification by frequency characteristics for long-term air quality prediction’, *Mathematics*, February, Vol. 8, No. 2, p.214.
- Leksmono, N.S., Longhurst, J.W.S., Ling, K.A., Chatterton, T.J., Fisher, B.E.A. and Irwin, J.G. (2006) ‘Assessment of the relationship between industrial and traffic sources contributing to air quality objective exceedances: a theoretical modelling exercise’, *Environmental Modelling & Software*, April, Vol. 21, No. 4, pp.494–500.
- Li, R., Dong, Y., Zhu, Z., Li, C. and Yang, H. (2019) ‘A dynamic evaluation framework for ambient air pollution monitoring’, *Applied Mathematical Modelling*, January, Vol. 65, pp.52–71.
- Li, X., Peng, L., Hu, Y., Shao, J. and Chi, T. (2016) ‘Deep learning architecture for air quality predictions’, *Environmental Science and Pollution Research*, Vol. 23, No. 22, pp.22408–22417.
- Lin, Y.C., Lee, S.J., Ouyang, C.S. and Wu, C.H. (2020) ‘Air quality prediction by neuro-fuzzy modeling approach’, *Applied Soft Computing*, January, Vol. 86, p.105898.

- Ma, J., Cheng, J.C., Lin, C., Tan, Y. and Zhang, J. (2019) 'Improving air quality prediction accuracy at larger temporal resolutions using deep learning and transfer learning techniques', *Atmospheric Environment*, October, Vol. 214, p.116885.
- Mao, W., Wang, W., Jiao, L., Zhao, S. and Liu, A. (2021) 'Modeling air quality prediction using a deep learning approach: method optimization and evaluation', *Sustainable Cities and Society*, February, Vol. 65, p.102567.
- Monn, C.H., Braendli, O., Schaeppi, G., Schindler, C., Ackermann-Liebrich, U., Leuenberger, P. and Sapaldia Team (1995) 'Particulate matter < 10 μm (PM10) and total suspended particulates (TSP) in urban, rural and alpine air in Switzerland', *Atmospheric Environment*, Vol. 29, No. 19, pp.2565–2573.
- Olvera-García, M.Á., Carbajal-Hernández, J.J., Sánchez-Fernández, L.P. and Hernández-Bautista, I. (2016) 'Air quality assessment using a weighted fuzzy inference system', *Ecological Informatics*, May, Vol. 33, pp.57–74.
- Schürholz, D., Kubler, S. and Zaslavsky, A. (2020) 'Artificial intelligence-enabled context-aware air quality prediction for smart cities', *Journal of Cleaner Production*, October, Vol. 271, p.121941.
- Turner, M.C., Krewski, D., Pope III, C.A., Chen, Y., Gapstur, S.M. and Thun, M.J. (2011) 'Long-term ambient fine particulate matter air pollution and lung cancer in a large cohort of never-smokers', *American Journal of Respiratory and Critical Care Medicine*, December, Vol. 184, No. 12, pp.1374–1381.
- Yan, J., Wang, L., Song, W., Chen, Y., Chen, X. and Deng, Z. (2019) 'A time-series classification approach based on change detection for rapid land cover mapping', *ISPRS Journal of Photogrammetry and Remote Sensing*, December, Vol. 158, pp.249–262.
- Yin, P., He, G., Fan, M., Chiu, K.Y., Fan, M., Liu, C., Xue, A., Liu, T., Pan, Y., Mu, Q. and Zhou, M. (2017) 'Particulate air pollution and mortality in 38 of China's largest cities: time series analysis', *BMJ*, March, Vol. 356.
- Zhang, L., Liu, P., Zhao, L., Wang, G., Zhang, W. and Liu, J. (2021) 'Air quality predictions with a semi-supervised bidirectional LSTM neural network', *Atmospheric Pollution Research*, January, Vol. 12, No. 1, pp.328–339.
- Zheng, Y., Liu, F. and Hsieh, H.P. (2013) 'U-air: when urban air quality inference meets big data', in *Proceedings of the 19th ACM SIGKDD International Conference on Knowledge Discovery and Data Mining*, August, pp.1436–1444.
- Zheng, Y., Yi, X., Li, M., Li, R., Shan, Z., Chang, E. and Li, T. (2015) 'Forecasting fine-grained air quality based on big data', in *Proceedings of the 21st ACM SIGKDD International Conference on Knowledge Discovery and Data Mining*, pp.2267–2276.
- Zhou, Q., Jiang, H., Wang, J. and Zhou, J. (2014) 'A hybrid model for PM2.5 forecasting based on ensemble empirical mode decomposition and a general regression neural network', *Science of the Total Environment*, Vol. 496, pp.264–274.